Supporting Information

Cyclometalated half-sandwich iridium(III) and rhodium(III) complexes as efficient agents against cancer stem-cell mammospheres

Dana Josa, [a] Piedad Herrera-Ramírez, [a] Xiao Feng, [b] Albert Gutiérrez, [a] David Aguilà, [a] Arnald Grabulosa, *[a] Manuel Martínez, [a] Kogularamanan Suntharalingam *[b] and Patrick Gamez *[acd]

Table of Contents

Table S1. Crystal data and structure refinement for compounds **1** and **1**·DMSO (CCDC 2390209 and 2390210, respectively).

Compound	**1**	**1**·DMSO
Empirical formula	$C_{38}H_{33}ClIrP$, CH_2Cl_2	$C_{40}H_{39}IrOPS$, F_6P, CH_2Cl_2
Formula weight (g mol^{-1})	833.19	1020.84
Temperature (K)	298	100
Crystal system	monoclinic	monoclinic
Space group	$P2_1/c$	$P2_1/c$
Crystal size (mm^3)	0.55 × 0.55 × 0.2	0.07 × 0.04 × 0.03
a (Å)	10.0487(2)	9.6150(19)
b (Å)	15.4228(4)	16.708(3)
c (Å)	21.9385(5)	24.477(5)
α (°)	90	90
β (°)	102.3600(10)	90.22(3)
γ (°)	90	90
V (Å^3)	3321.20(13)	3932.1(14)
Z	4	4
ρ_{calcd}	1.666	1.724
μ (mm^{-1})	4.338	3.967
F(000)	1648	2024
ϑ for data collection (°)	1.627– 28.725	1.514– 29.522
Reflections collected / unique	32794 / 8593	62263 / 9527
Completeness to theta	1.000	0.953
Data / restraints / parameters	8593 / 42 / 421	9527 / 0 / 467
Goodness-of-fit on F^2	1.058	1.086
Final R indices [$I>2\sigma(I)$]	R1 = 0.0258, wR2 = 0.0609	R1 = 0.0226, wR2 = 0.0612
R indices (all data)	R1 = 0.0314, wR2 = 0.0630	R1 = 0.0231, wR2 = 0.0615
largest diff. peak and hole (e Å^3)	0.445 and −1.754	1.000 and −1.998

Table S2. Selected bond distances (Å) and angles (°) for compounds **1**, **1**·DMSO and **2**·DMSO. Representations of the solid-state structures of these compounds are shown in Figures 1 and S2, respectively. *C* stands for the centroid of the Cp* ligand.

1			
Ir–Cl1	2.4074(7)	Cl1–Ir–P1	89.86(3)
Ir–P1	2.2585(7)	P1–Ir–C1	81.60(7)
Ir–C1	2.070(2)	C1–Ir–Cl1	82.37(7)
Ir–*C*	1.8725(13)	Cl1–Ir–*C*	122.56(5)
		P1–Ir–*C*	132.84(5)
		C1–Ir–*C*	131.34(9)
1·DMSO			
Ir–S1	2.2897(8)	S1–Ir–P1	96.47(3)
Ir–P1	2.2963(8)	P1–Ir–C1	82.18(6)
Ir–C1	2.076(2)	C1–Ir–S1	82.54(6)
Ir–*C*	1.9057(11)	S1–Ir–*C*	123.96(4)
		P1–Ir–*C*	130.49(4)
		C1–Ir–*C*	126.17(7)
2·DMSO			
Rh–S1	2.3141(7)	S1–Rh–P1	97.08(3)
Rh–P1	2.3054(8)	P1–Rh–C7	82.47(6)
Rh–C7	2.064(2)	C7–Rh–S1	82.40(6)
Rh–*C*	1.8968(11)	S1–Rh–*C*	124.07(4)
		P1–Rh–*C*	129.91(4)
		C7–Rh–*C*	126.07(7)

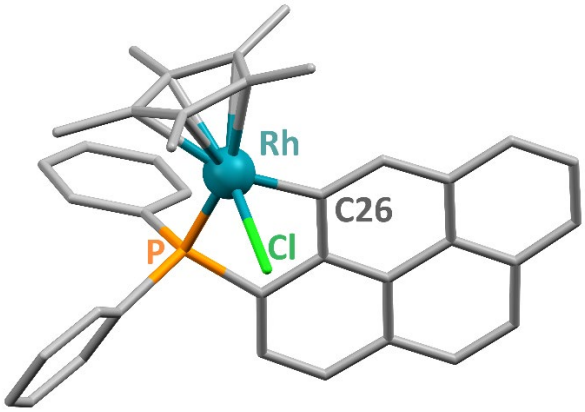

Figure S1. Representation of the solid-state structure of **2**.[1] The donor atoms coordinated to the metal centre are labelled. Hydrogen atoms are omitted for clarity.

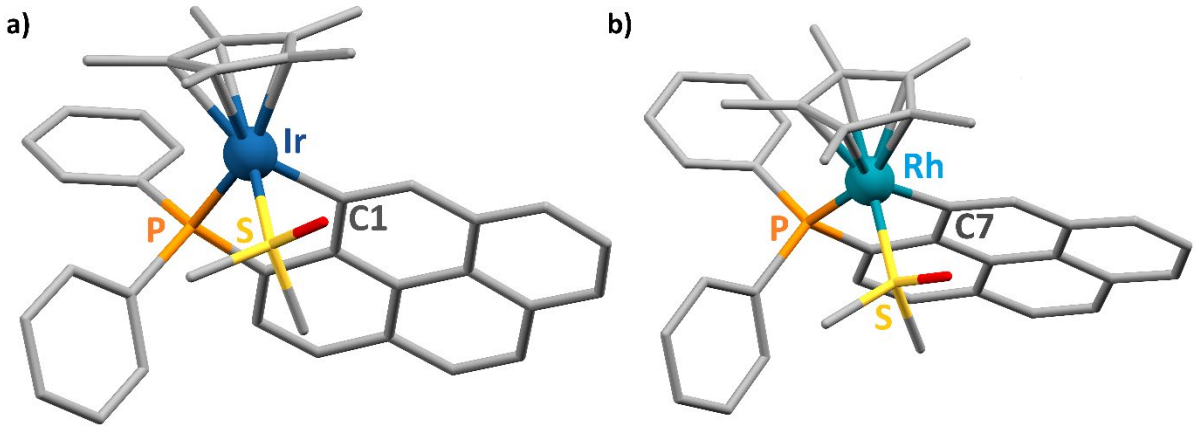

Figure S2. Representations of the solid-state structures of a) **1**·DMSO and b) **2**·DMSO. The donor atoms coordinated to the metal centre are labelled. Hydrogen atoms are omitted for clarity.

Table S3. Crystal data and structure refinement for compound **2**·DMSO (CCDC 2390211).

Compound	**2**·DMSO
Empirical formula	$C_{40}H_{39}OPRhS$, F_6P, CH_2Cl_2
Formula weight (g mol^{-1})	931.55
Temperature (K)	100
Crystal system	monoclinic
Space group	$P2_1/c$
Crystal size (mm^3)	0.13 × 0.05 × 0.05
a (Å)	9.6550(19)
b (Å)	16.670(3)
c (Å)	24.415(5)
α (°)	90
β (°)	90.21(3)
γ (°)	90
V (Å^3)	3929.5(14)
Z	4
ρ_{calcd}	1.575
μ (mm^{-1})	0.816
F(000)	1896
ϑ for data collection (°)	1.518– 29.520
Reflections collected / unique	64275 / 9548
Completeness to theta	0.954
Data / restraints / parameters	9548 / 0 / 467
Goodness-of-fit on F^2	1.160
Final R indices [$I>2\sigma(I)$]	R1 = 0.0427, wR2 = 0.1215
R indices (all data)	R1 = 0.0428, wR2 = 0.1216
largest diff. peak and hole (e Å^3)	1.304 and −1.826

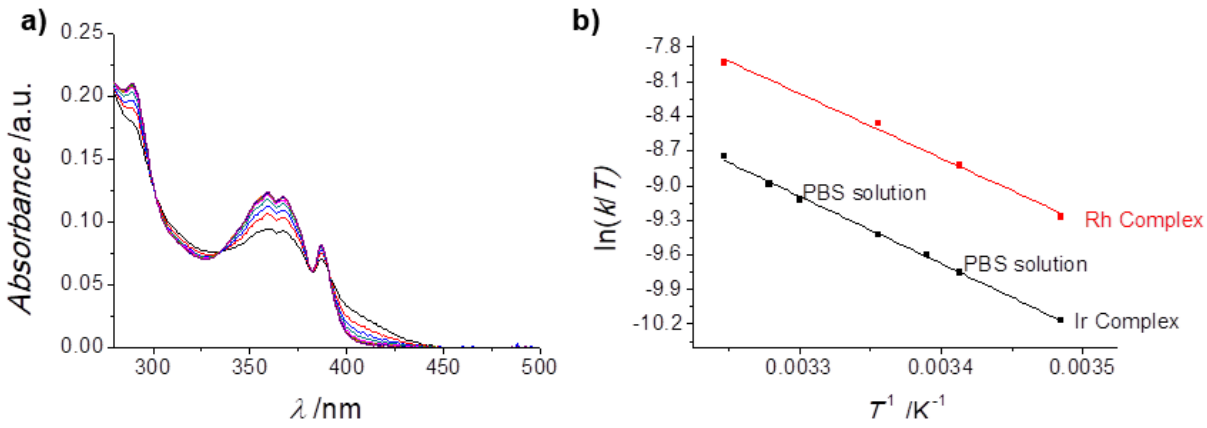

Figure S3. a) UV-Vis time-resolved spectral changes of a 20% DMSO aqueous solution of **2** (10 μM) recorded at 25 °C for 4 minutes, in the range 600–280 nm. b) Eyring plots for the temperature dependence of the reactions of 10 μM 20 % DMSO aqueous solution of **1** and **2**.

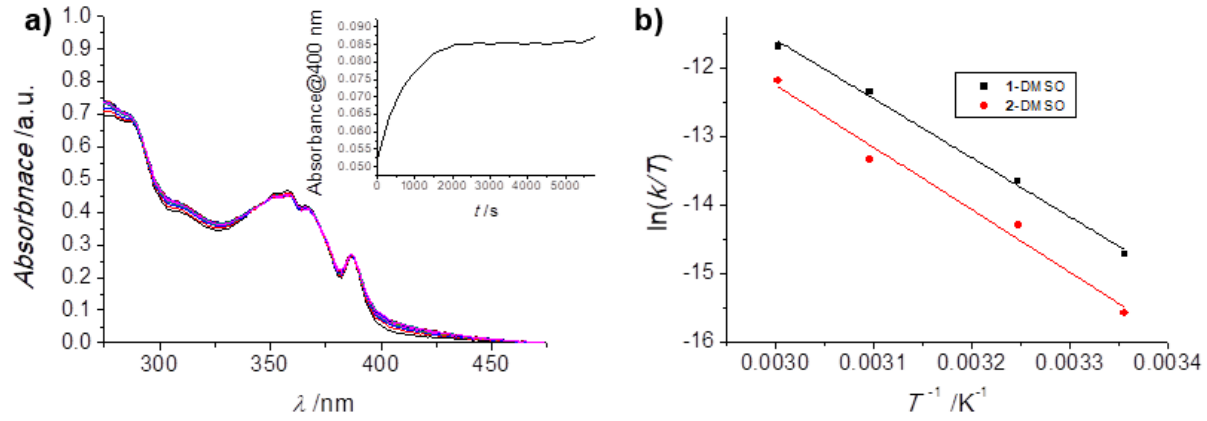

Figure S4. a) UV-Vis time-resolved spectral changes of a 20% DMSO aqueous solution of **1**-DMSO at 50 °C. b) Eyring plots for the temperature dependence of the reactions of 5-10 μM 20 % DMSO aqueous solution of **1**-DMSO and **2**-DMSO.

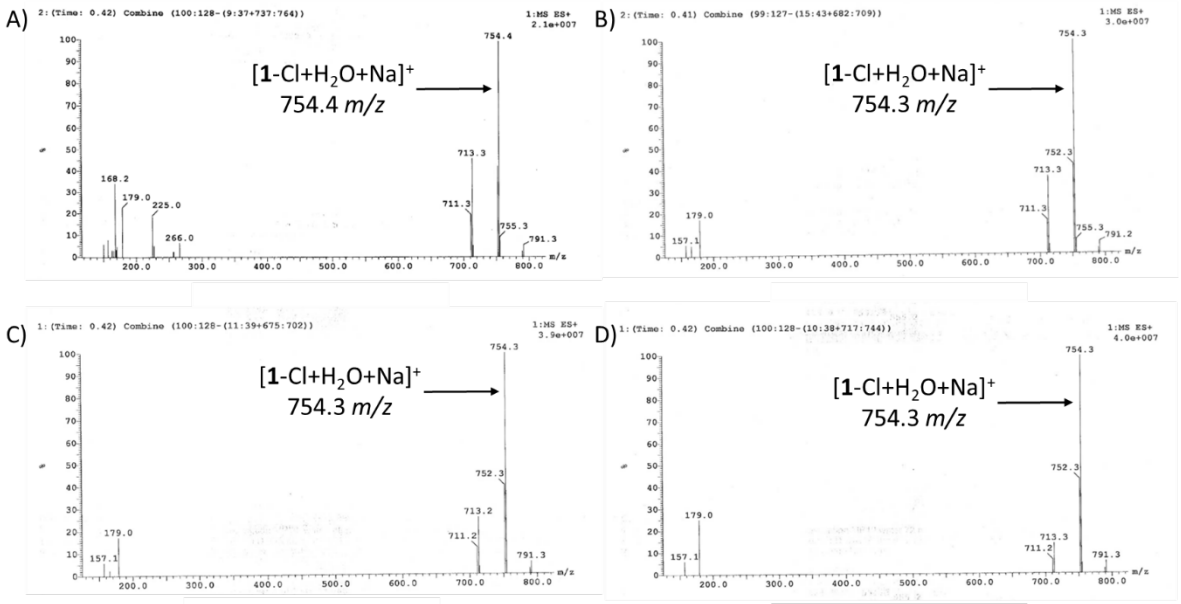

Figure S5. ESI mass spectra (positive mode) of **1** (500 μM) in H_2O:DMSO (5:1) after incubation for (A) 0 h, (B) 24 h, (C) 48 h or (D) 72 h at 37 °C.

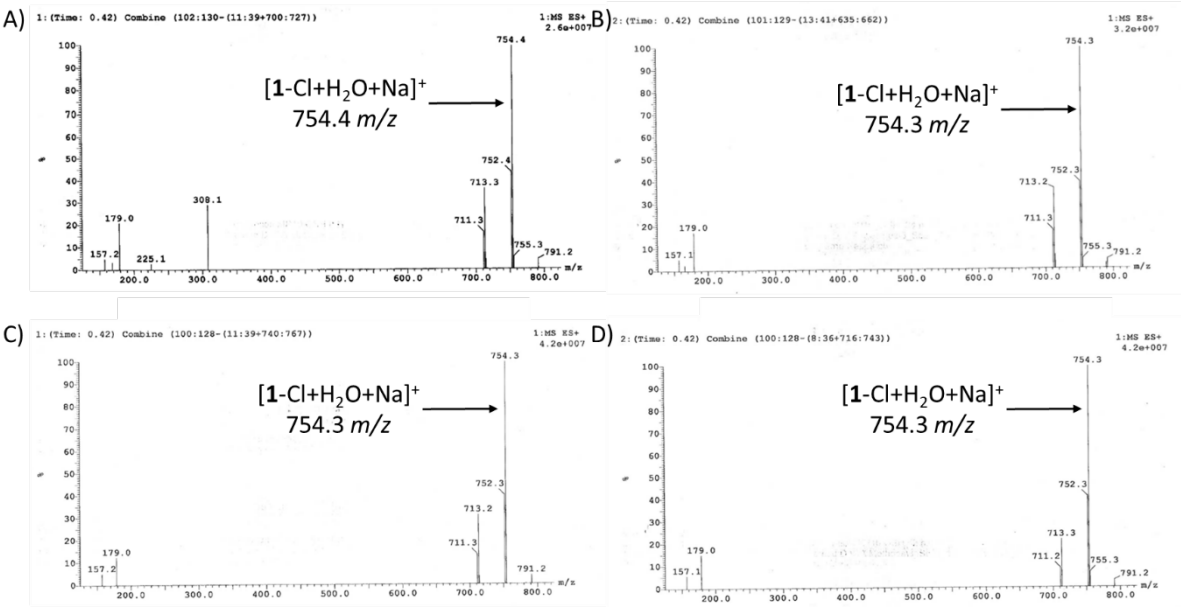

Figure S6. ESI mass spectra (positive mode) of **1** (500 μM) in H_2O:DMSO (5:1) in the presence of glutathione (500 μM) after incubation for (A) 0 h, (B) 24 h, (C) 48 h or (D) 72 h at 37 °C.

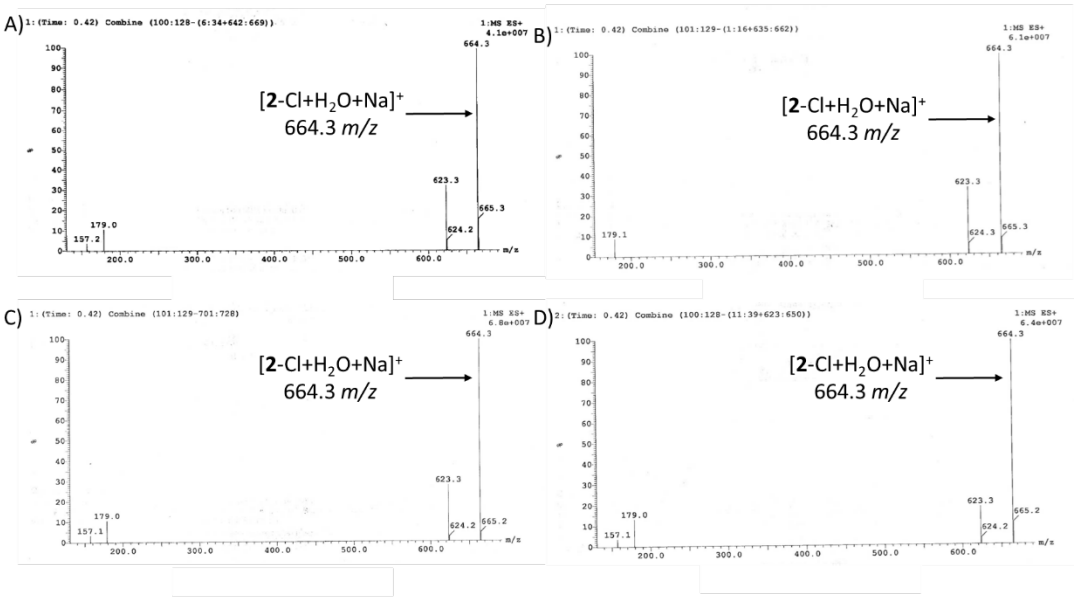

Figure S7. ESI mass spectra (positive mode) of **2** (500 μM) in H_2O:DMSO (5:1) after incubation for (A) 0 h, (B) 24 h, (C) 48 h or (D) 72 h at 37 °C.

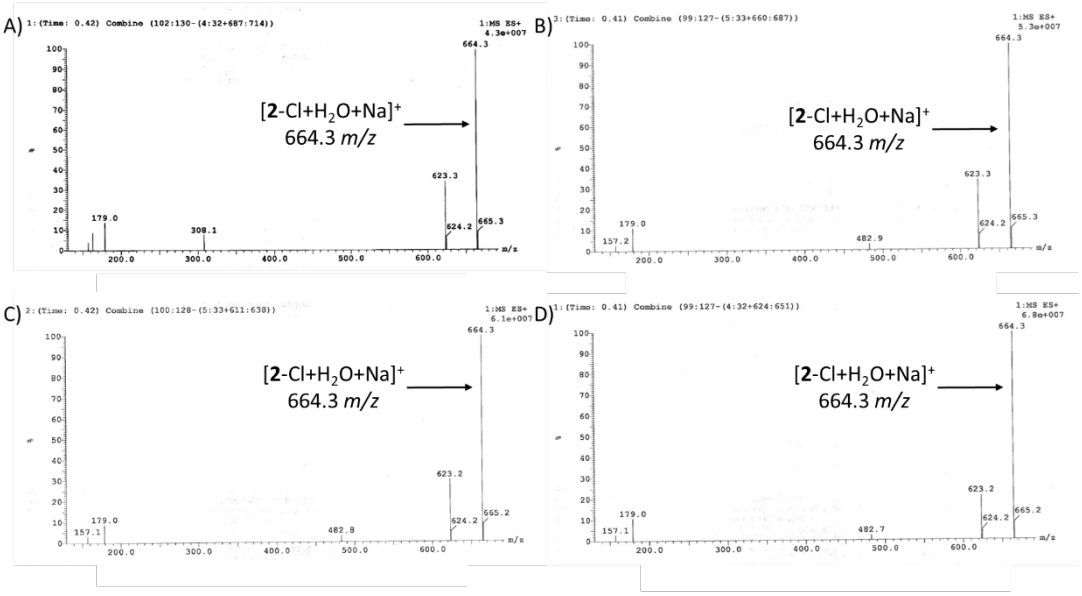

Figure S8. ESI mass spectra (positive mode) of **2** (500 μM) in H_2O:DMSO (5:1) in the presence of glutathione (500 μM) after incubation for (A) 0 h, (B) 24 h, (C) 48 h or (D) 72 h at 37 °C.

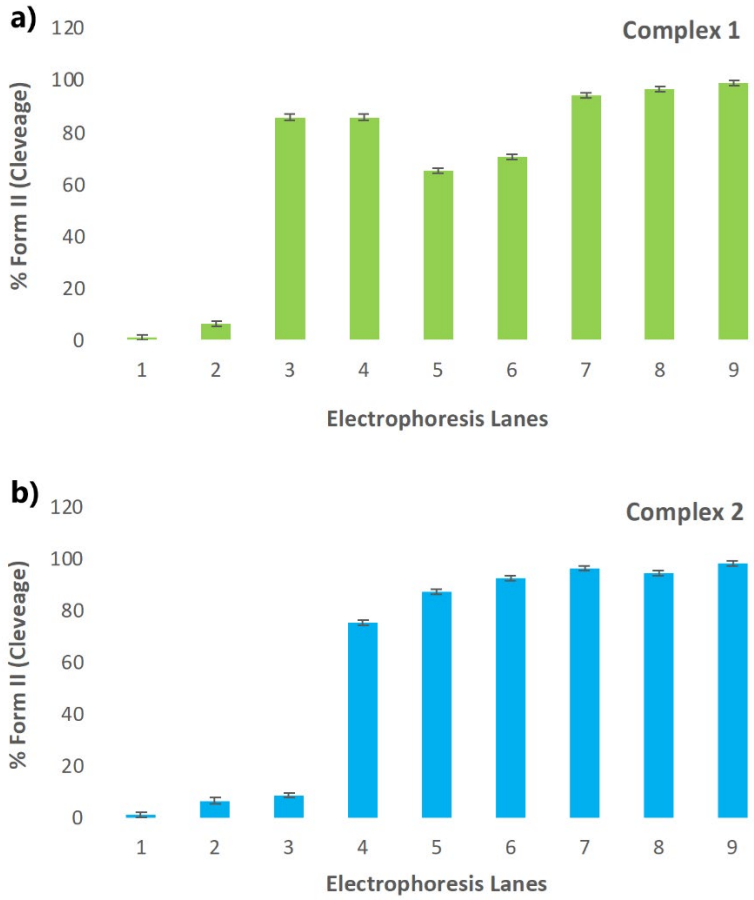

Figure S9. Percentages of DNA Form II (nicked/open circle) detected in the different gel electrophoresis lanes (see caption of Figure 2 in the main text for the conditions used in each lane) for a) complex **1** (in green) and b) complex **2** (in blue).

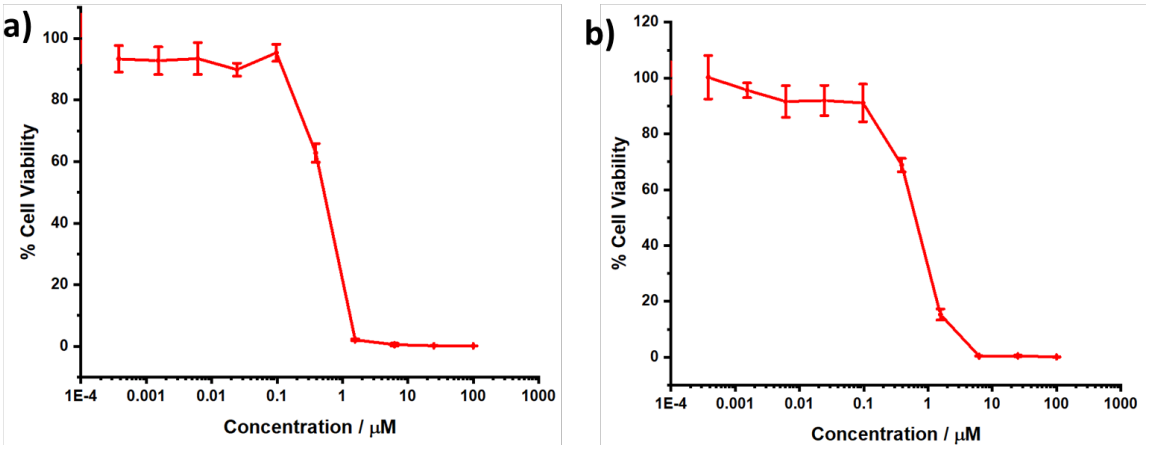

Figure S10. Representative dose-response curves for the treatment of HMLER cells with a) **1** and b) **2** after 72 h incubation.

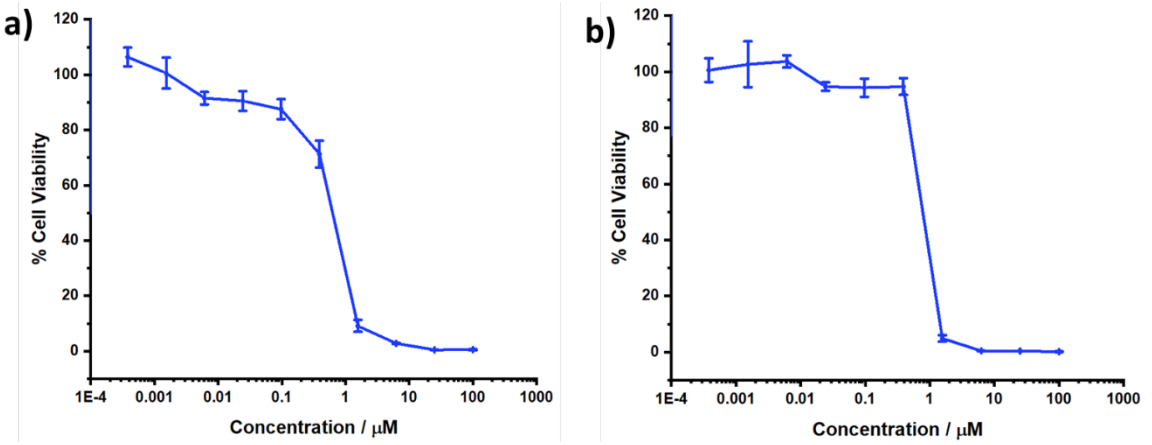

Figure S11. Representative dose-response curves for the treatment of HMLER-shEcad cells with a) **1** and b) **2** after 72 h incubation.

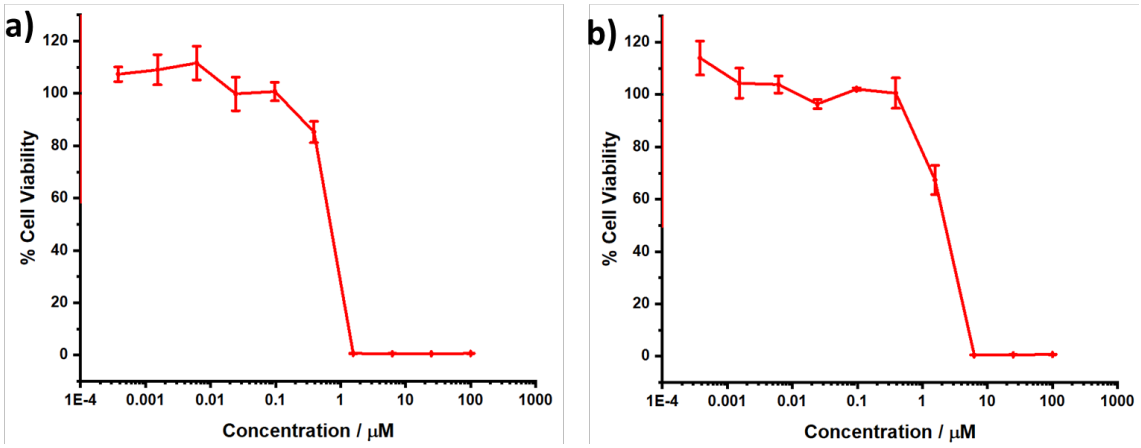

Figure S12. Representative dose-response curves for the treatment of BEAS-2B cells with a) **1** and b) **2** after 72 h incubation.

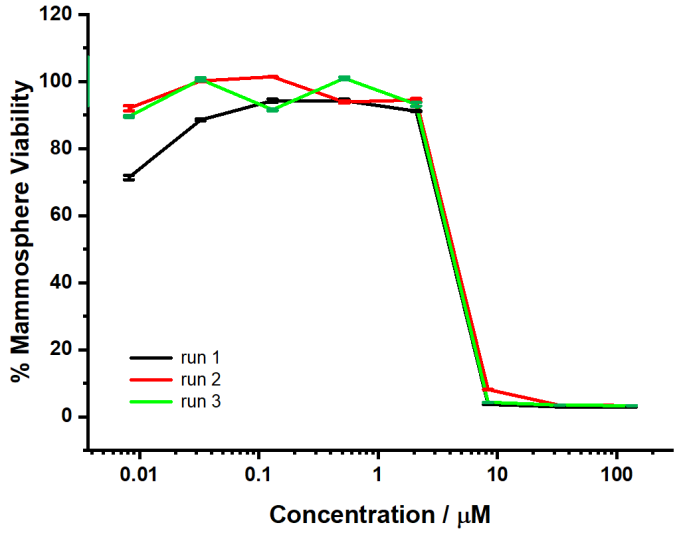

Figure S13. Representative dose-response curves for the treatment of HMLER-shEcad mammospheres with **1** after 5 days incubation.

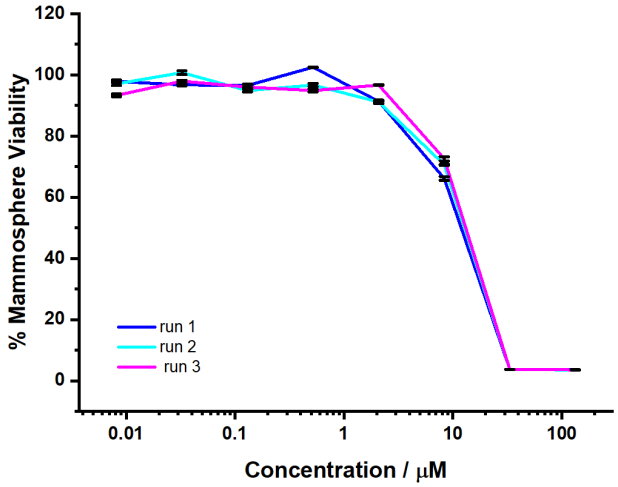

Figure S14. Representative dose-response curves for the treatment of HMLER-shEcad mammospheres with **2** after 5 days incubation.

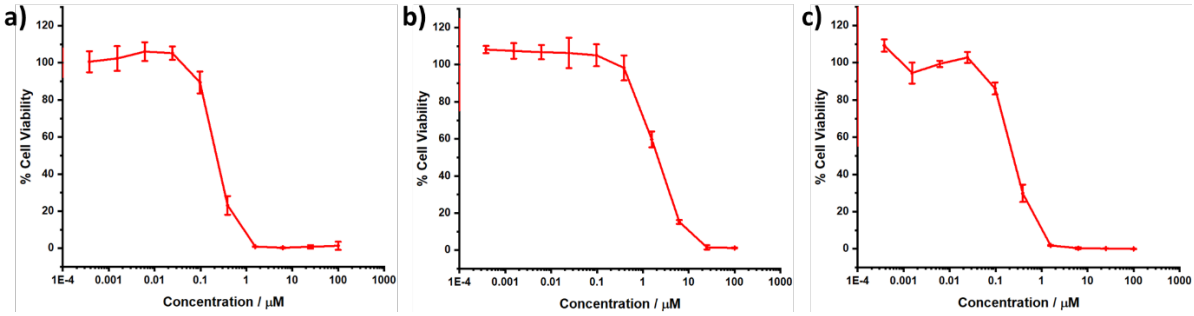

Figure S15. Representative dose-response curves for the treatment of HMLER-shEcad cells with **1** in the presence of a) IM-54 (10 μM), b) necrostatin-1 (20 μM) or c) z-VAD-FMK (5 μM).

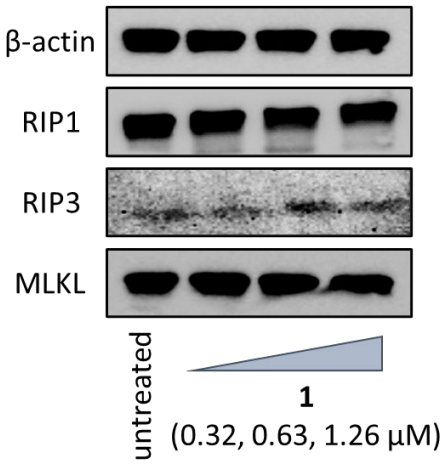

Figure S16. Immunoblotting analysis of proteins related to the necroptosis pathway. Protein expression in HMLER-shEcad cells following treatment with **1** (0.32, 0.63, and 1.26 μM) after 72 h incubation.

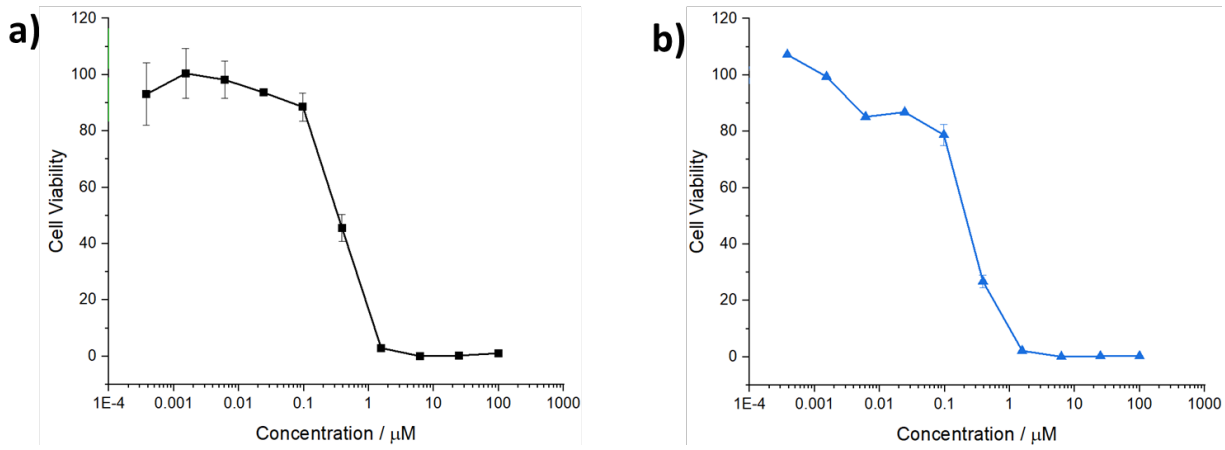

Figure S17. Representative dose-response curves for the treatment of HMLER-shEcad cells with **1** in the presence of a) ABT-888 (10 µM) or b) ANA (10 µM).

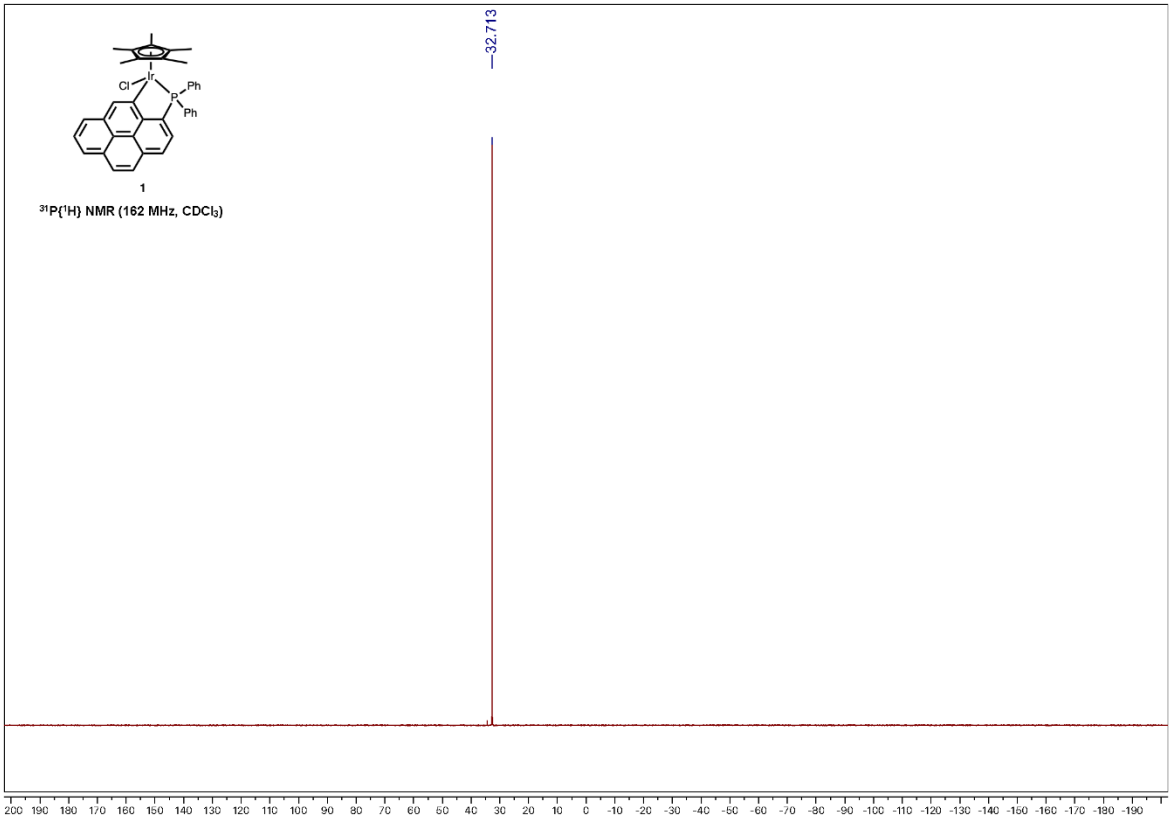

Figure S18. $^{31}P\{^{1}H\}$c NMR spectrum of **1** in $CDCl_3$.

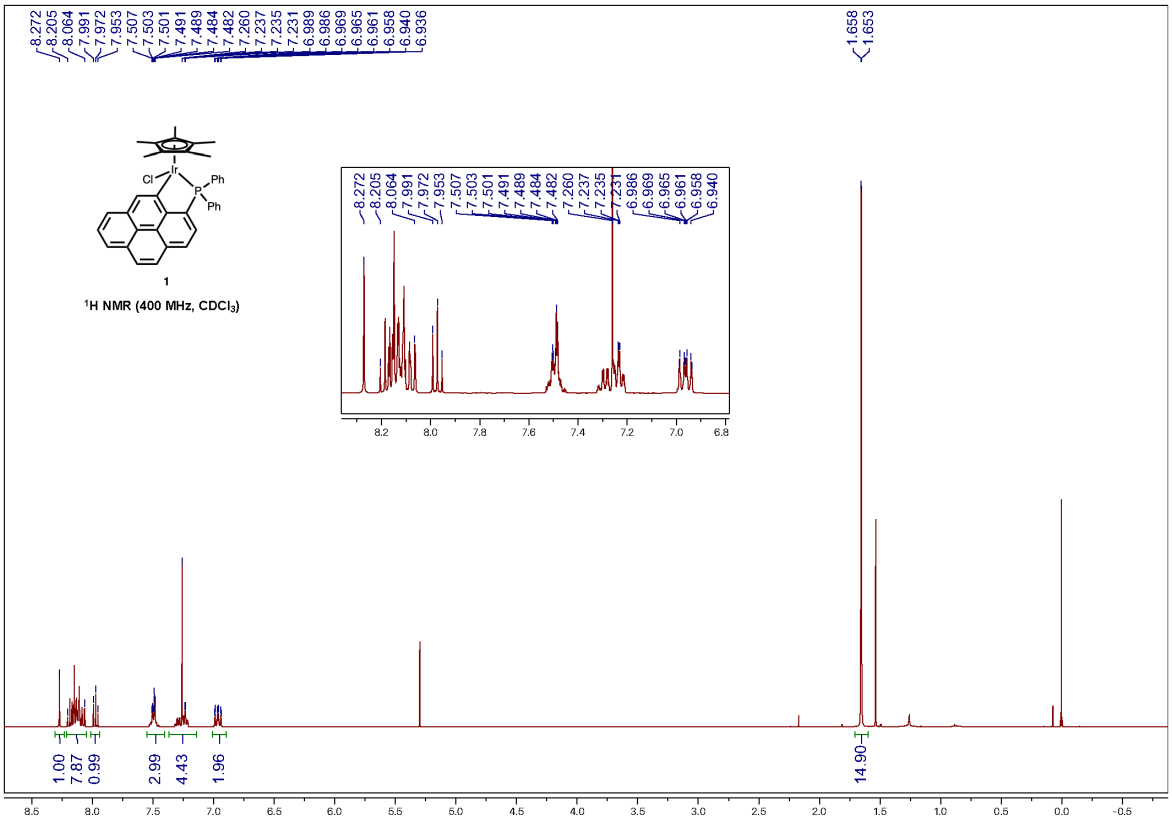

Figure S19. ^{1}H NMR spectrum of **1** in $CDCl_3$.

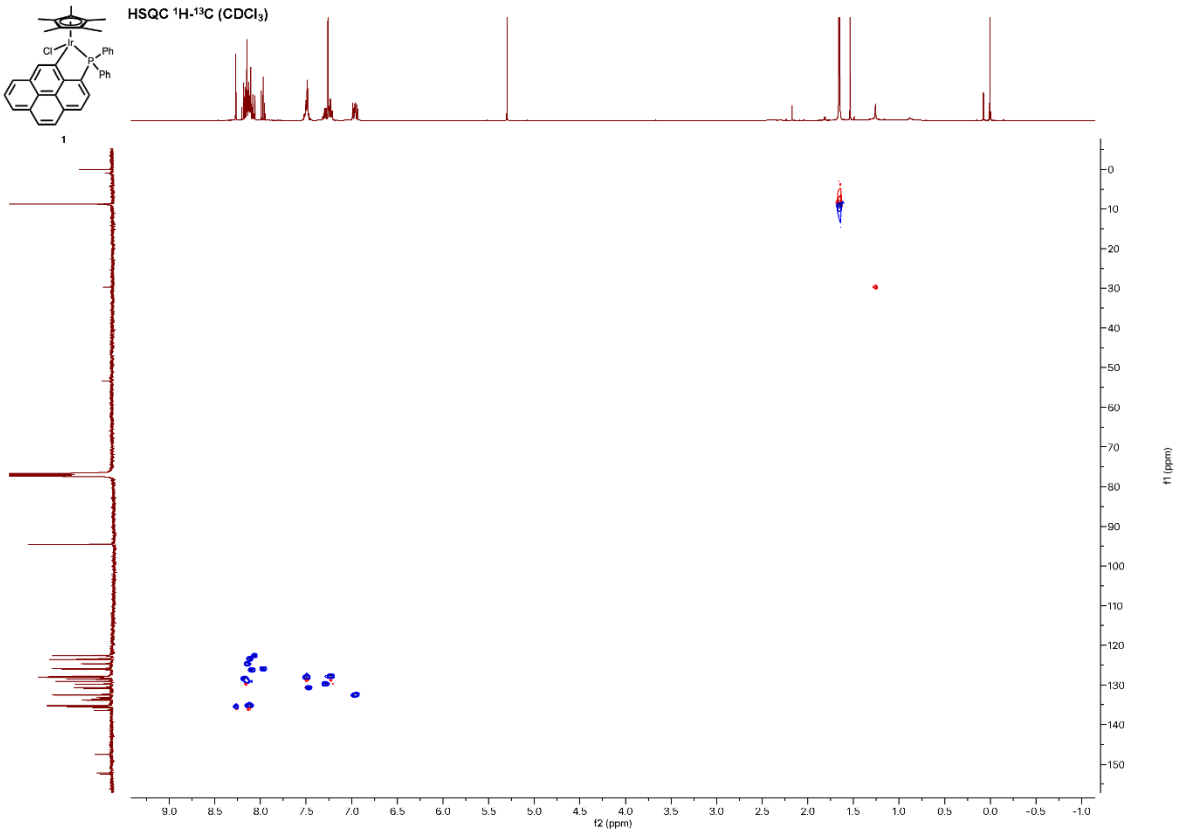

Figure S20. ^{1}H-^{13}C HSQC NMR spectrum of **1** in $CDCl_3$.

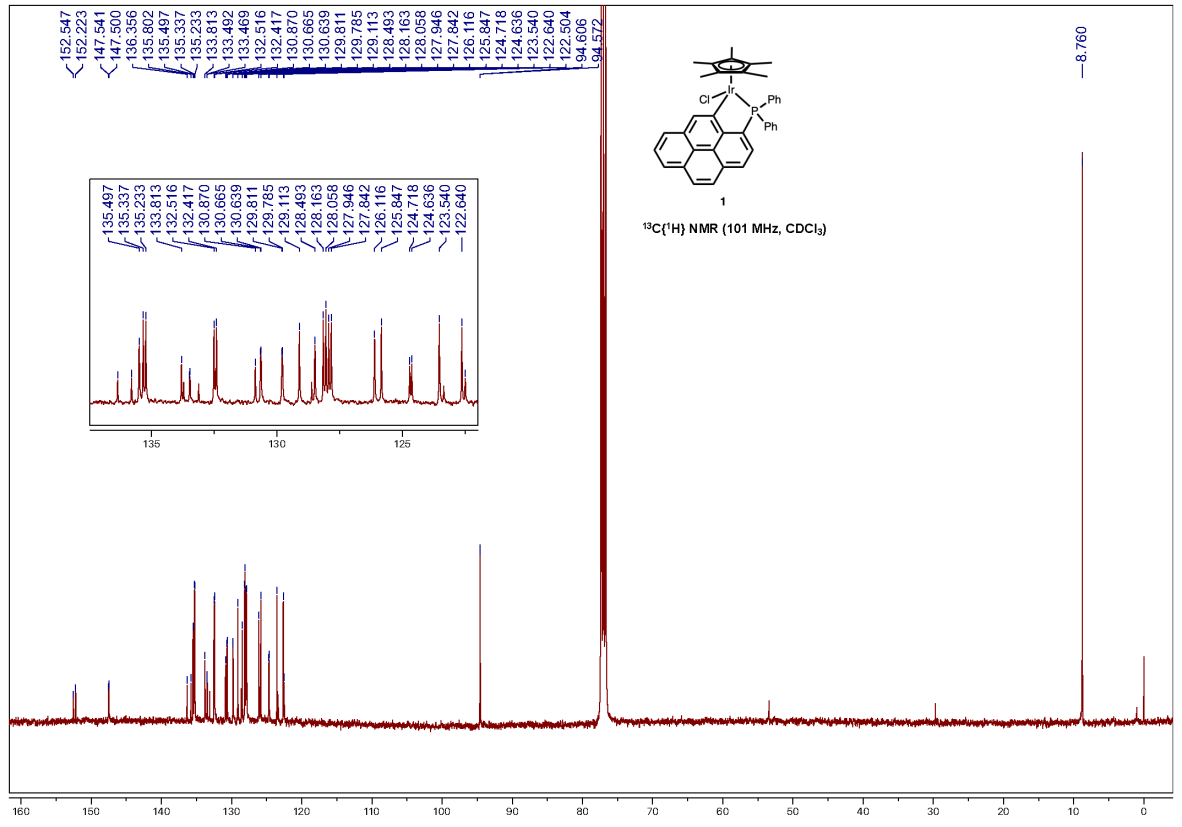

Figure S21. ^{13}C NMR spectrum of **1** in $CDCl_3$.

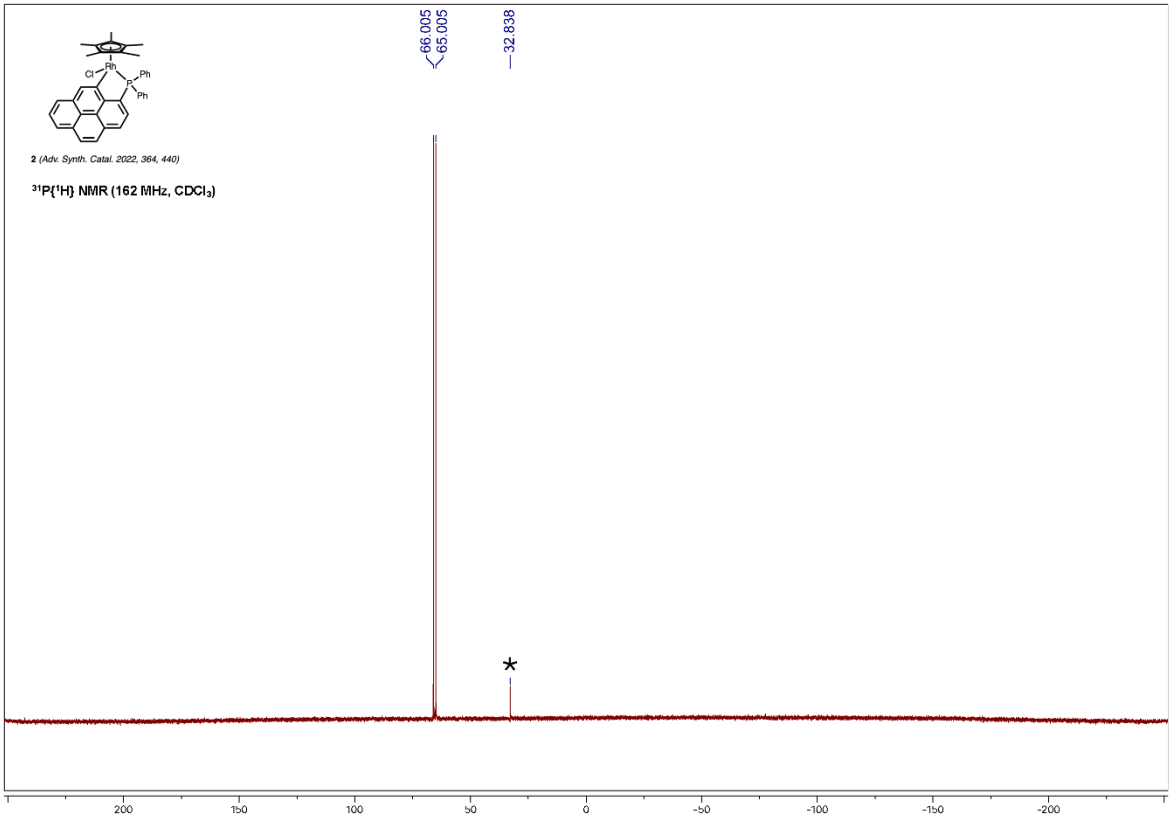

Figure S22. $^{31}P\{^{1}H\}$ NMR spectrum of **2** in $CDCl_3$. *: traces of the oxide of the free phosphane ligand.

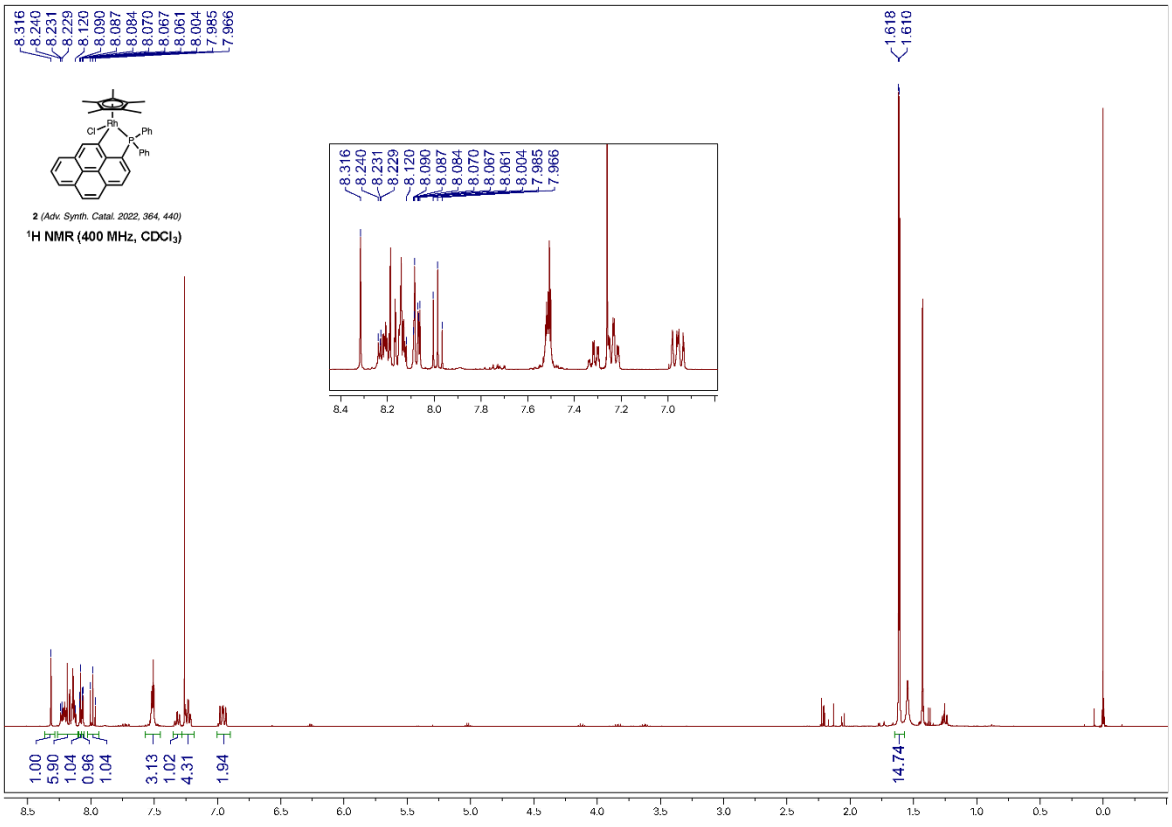

Figure S23. ^{1}H NMR spectrum of **2** in $CDCl_3$.

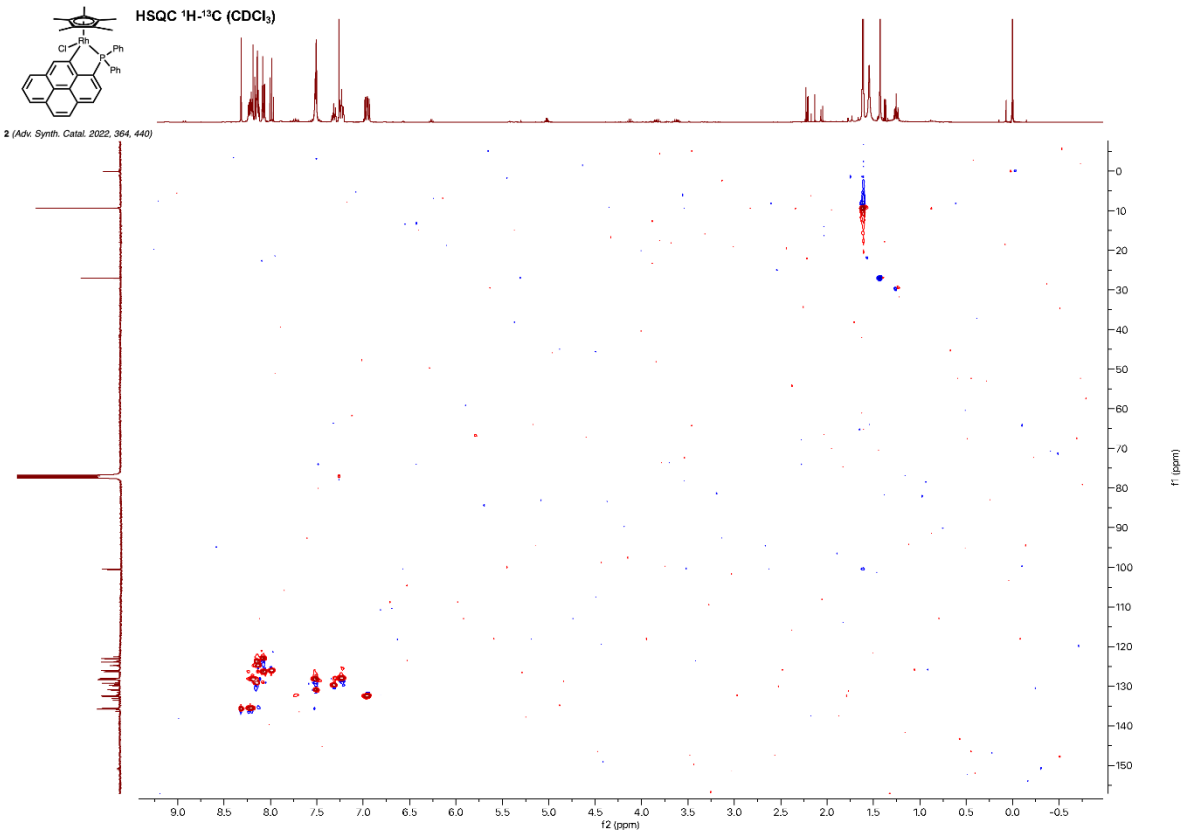

Figure S24. ^{1}H-^{13}C HSQC NMR spectrum of **2** in $CDCl_3$.

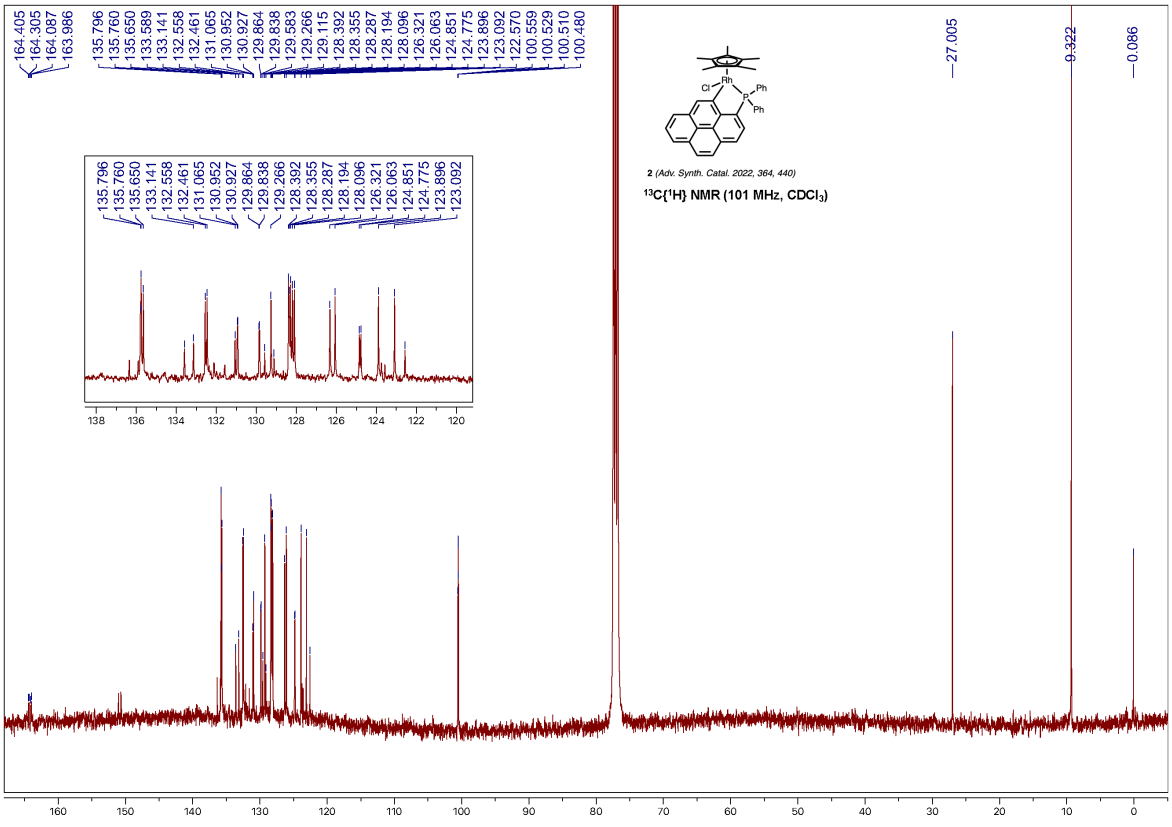

Figure S25. ^{13}C NMR spectrum of **2** in $CDCl_3$.

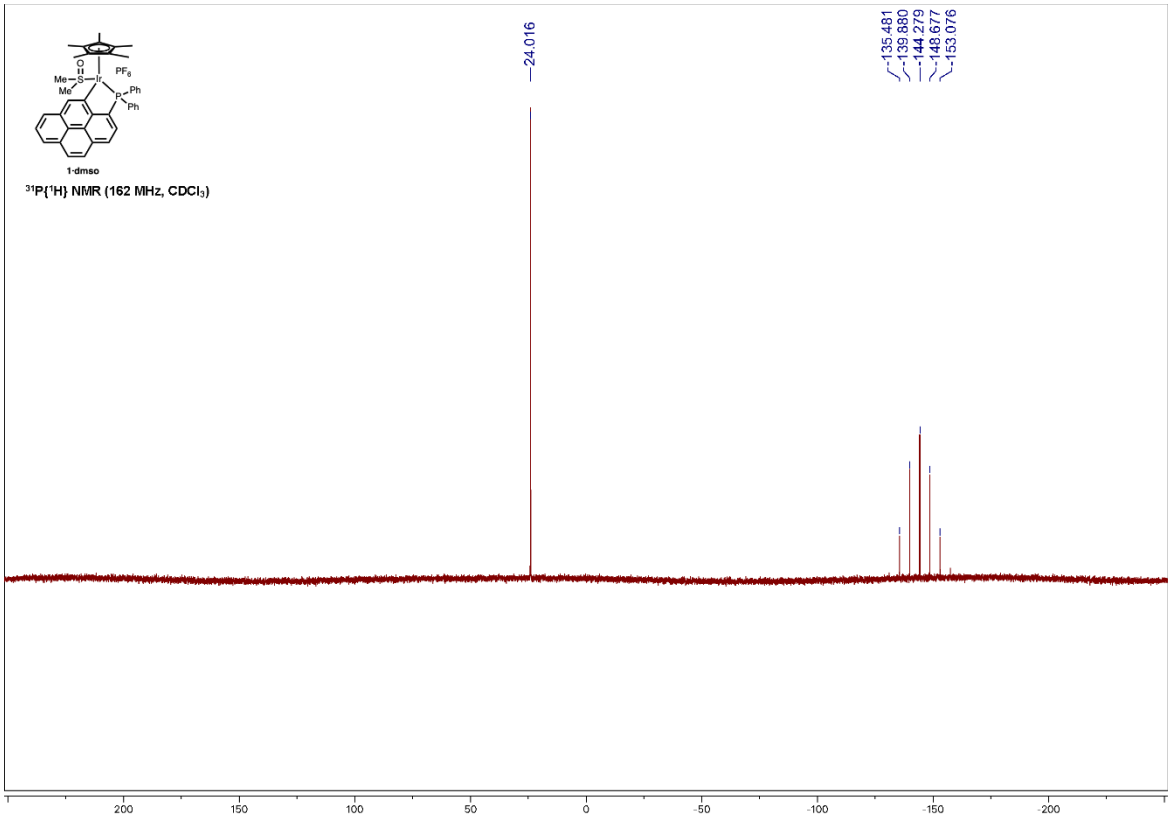

Figure S26. $^{31}P\{^{1}H\}$ NMR spectrum of **1**·DMSO in $CDCl_3$.

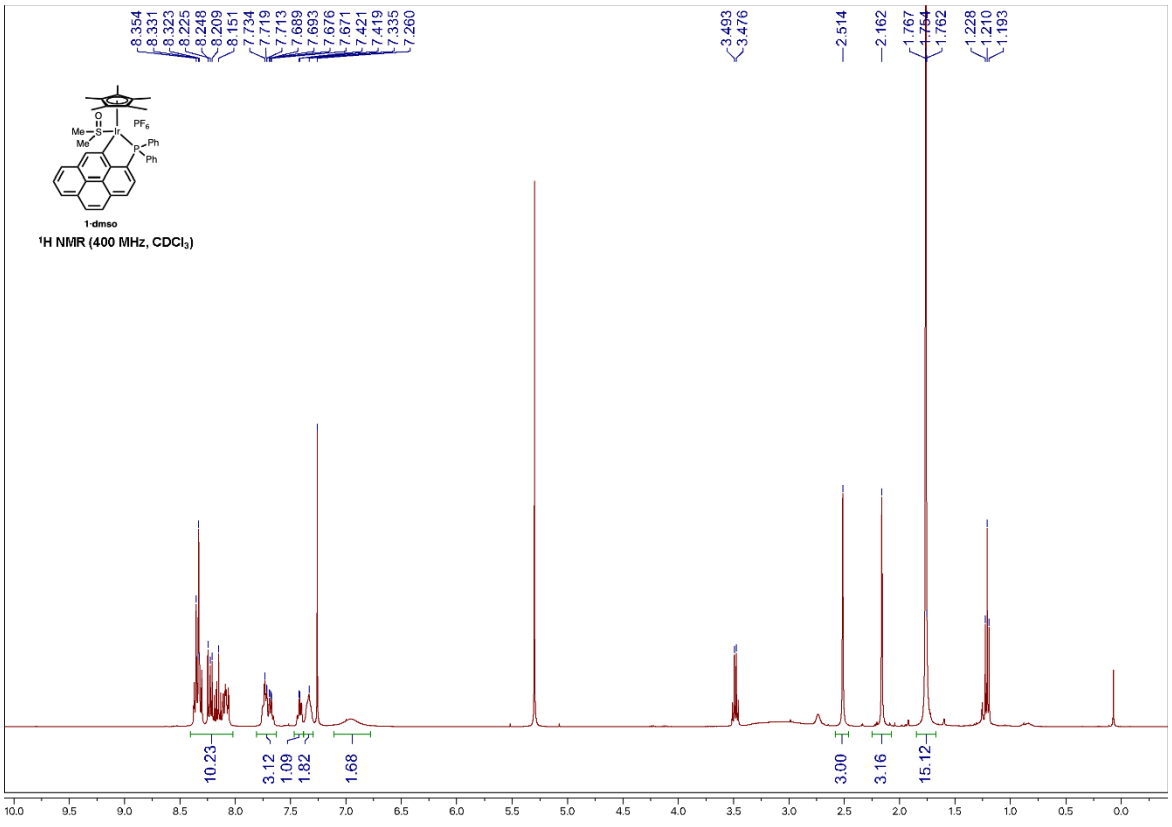

Figure S27. ^{1}H NMR spectrum of **1**·DMSO in $CDCl_3$.

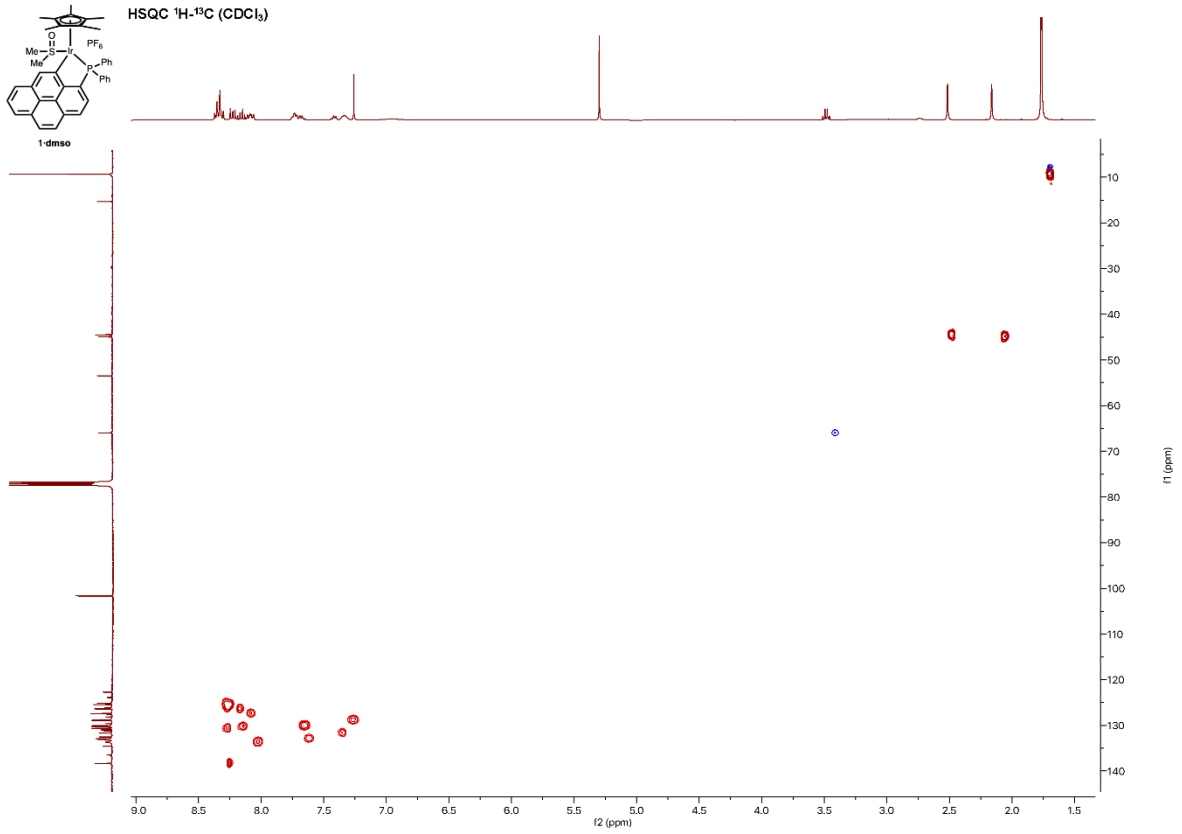

Figure S28. ^{1}H-^{13}C HSQC NMR spectrum of **1**·DMSO in $CDCl_3$.

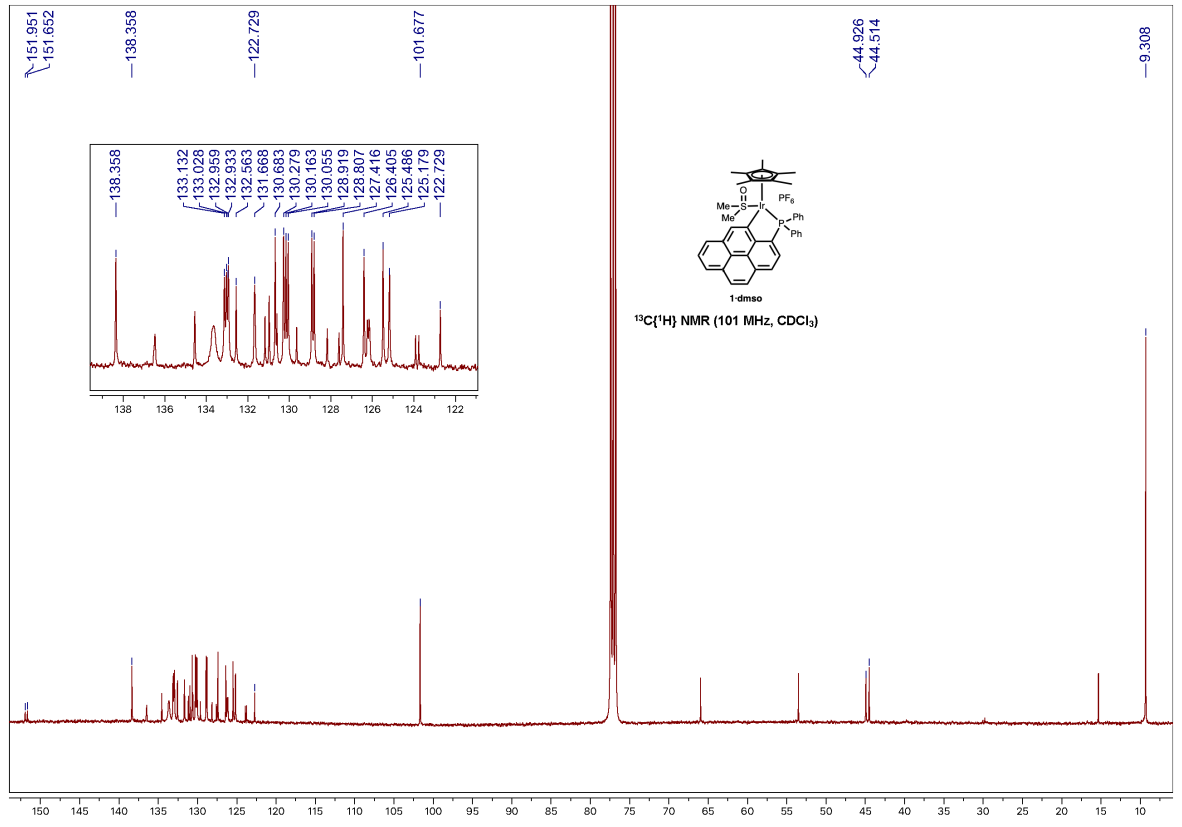

Figure S29. ^{13}C NMR spectrum of **1**·DMSO in $CDCl_3$.

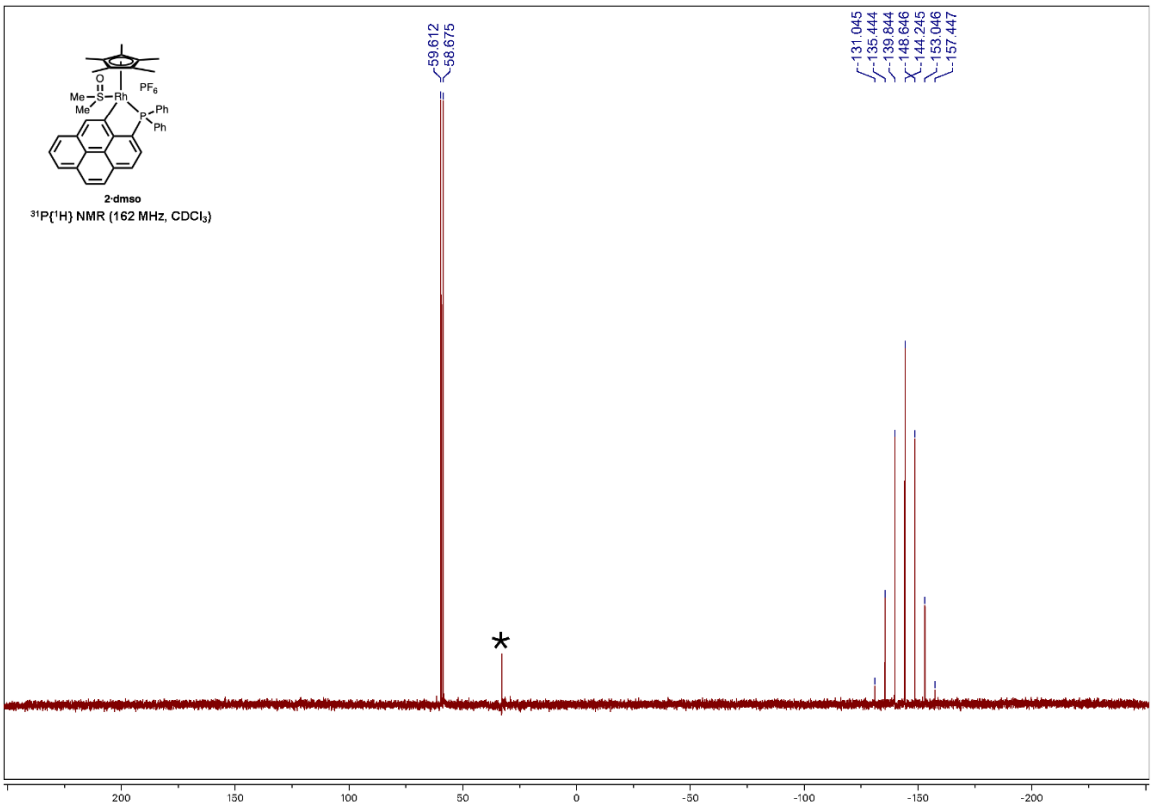

Figure S30. $^{31}P\{^{1}H\}$ NMR spectrum of **2**·DMSO in $CDCl_3$. *: traces of the oxide of the free phosphane ligand.

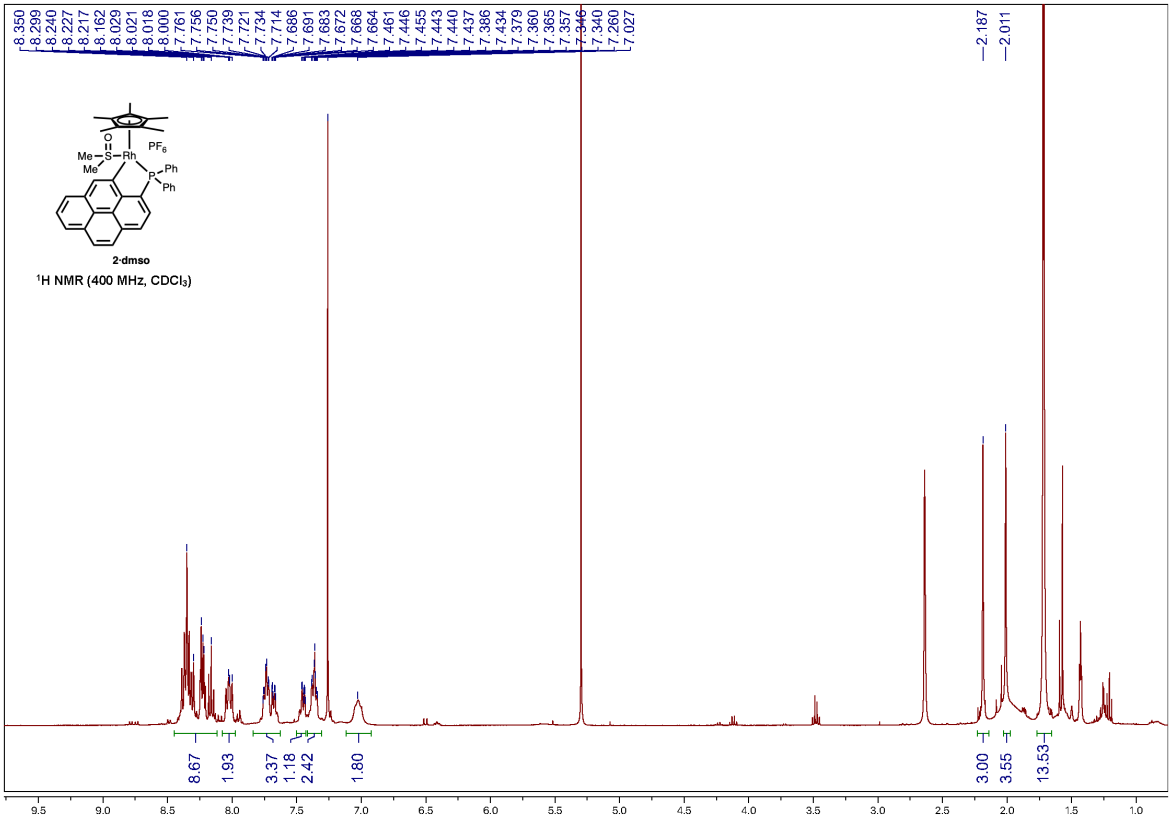

Figure S31. ^{1}H NMR spectrum of **2**·DMSO in $CDCl_3$.

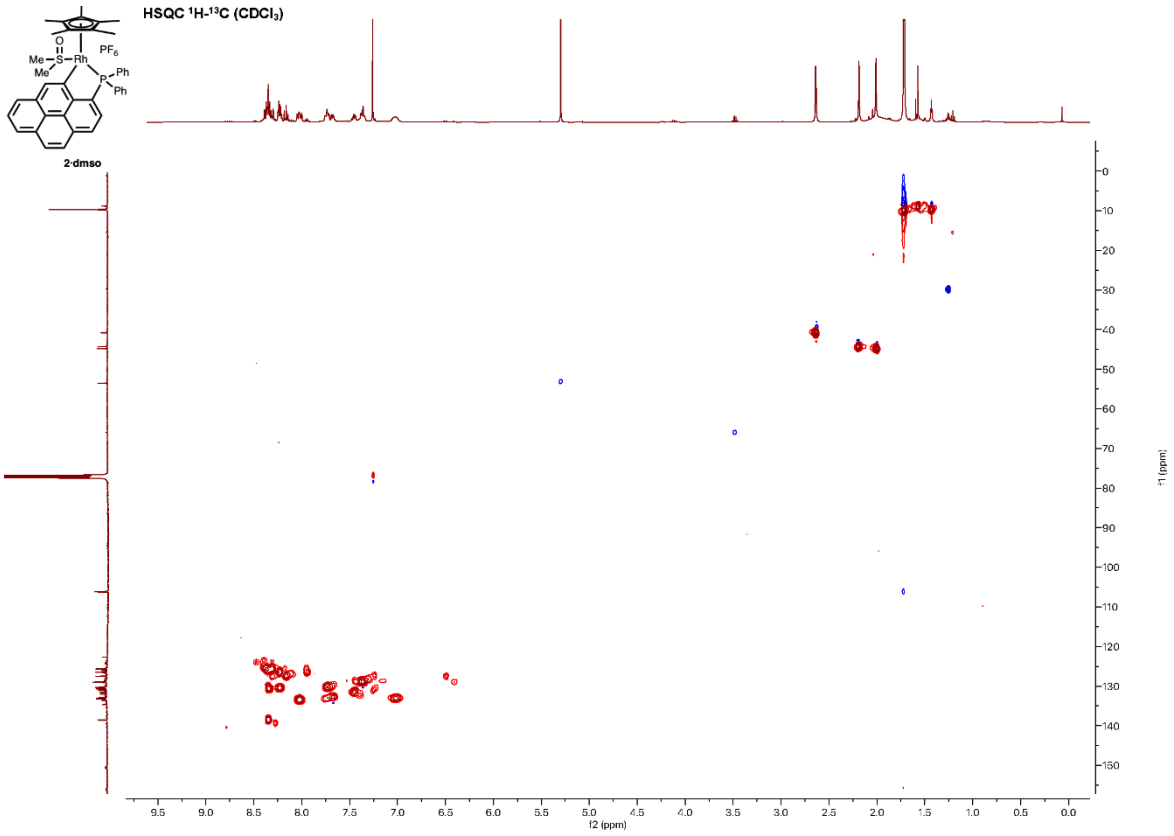

Figure S32. ^{1}H-^{13}C HSQC NMR spectrum of **2**·DMSO in $CDCl_3$.

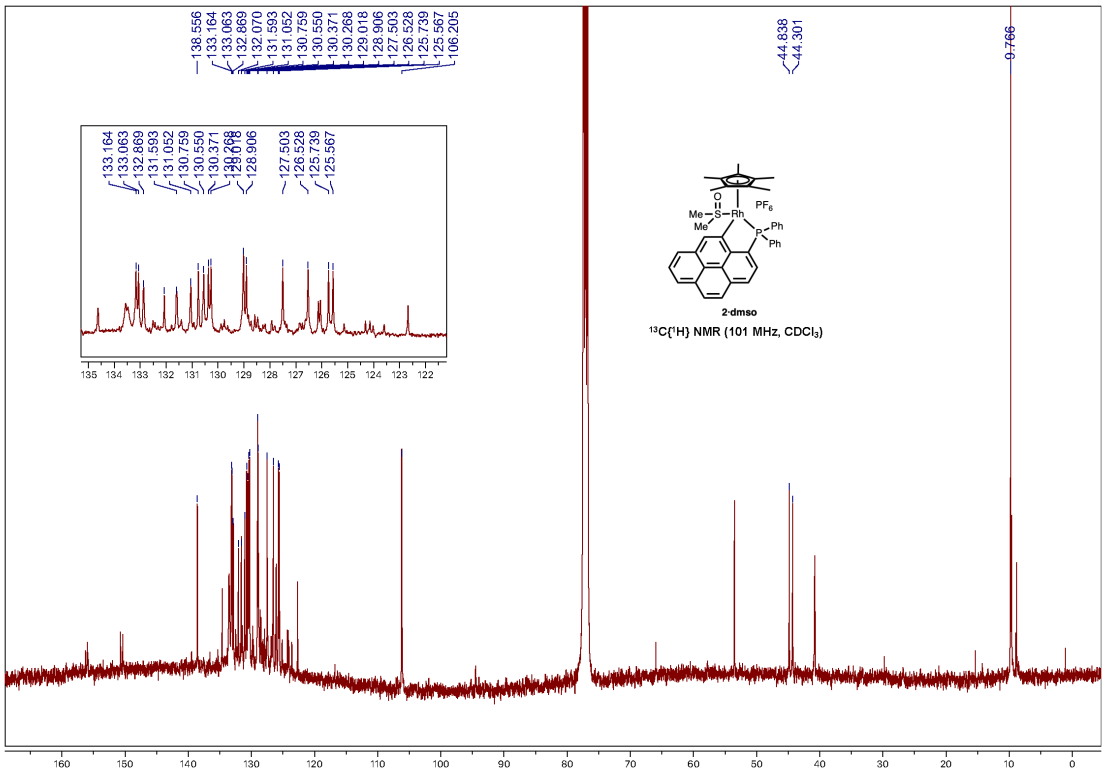

Figure S33. ^{13}C NMR spectrum of **2**·DMSO in $CDCl_3$.

References

1. C. Sire, H. Cattey, A. Tsivery, J. C. Hierso and J. Roger, Phosphorus-Directed Rhodium-Catalyzed C-H Arylation of 1-Pyrenylphosphines Selective at the K-Region, *Adv. Synth. Catal.*, 2022, **364**, 440-452.